J. Membrane Biol. 77, 223–241 (1984)

The Journal of
Membrane Biology

X-ray Microanalysis of Elements in Frozen-Hydrated Sections of an Electrogenic K^+ Transport System: The Posterior Midgut of Tobacco Hornworm (*Manduca sexta*) *in Vivo* and *in Vitro*

Julian A.T. Dow*†, Brij L. Gupta, Theodore A. Hall, and William R. Harvey*

Biological Microprobe Laboratory, Department of Zoology, University of Cambridge, Cambridge, CB2 3EJ, United Kingdom and
* Department of Biology, Temple University, Philadelphia, Pennsylvania 19122

Summary. The lepidopteran midgut is a model for the oxygen-dependent, electrogenic K^+ transport found in both alimentary and sensory tissues of many economically important insects. Structural and biochemical evidence places the K^+ pump on the portasome-studded apical plasma membrane which borders the extracellular goblet cavity. However, electrochemical evidence implies that the goblet cell K^+ concentration is less than 50 mM. We used electron probe X-ray microanalysis of frozen-hydrated cryosections to measure the concentration of Na, Mg, P, S, Cl, K, Ca and H_2O in several subcellular sites in the larval midgut of *Manduca sexta* under several experimental regimes. Na is undetectable at any site. K is at least 100 mM in the cytoplasm of all cells. Typical *in vivo* values (mM) for K were: blood, 25; goblet and columnar cytoplasm, 120; goblet cavity, 190; and gut lumen, 180. The high K concentration in the apically located goblet cavity declined by 100 mM under anoxia. Both cavity and gut fluid are Cl deficient, but fixed negative charges may be present in the cavity. We conclude that the K^+ pump is sited on the goblet cell apical membrane and that K^+ follows a nonmixing pathway via only part of the goblet cell cytoplasm. The cavity appears to be electrically isolated in alimentary tissues, as it is in sensory sensilla, thereby allowing a PD exceeding 180 mV (lumen positive) to develop across the apical plasma membrane. This PD appears to couple K^+ pump energy to nutrient absorption and pH regulation.

Key Words X-ray microanalysis · frozen-hydrated cryosections · electrogenic K^+ pump · K^+ ATPase · pH alkalization · chemiosmosis · extracellular matrices

Introduction

A Na^+ independent, electrogenic K^+ pump is present in epithelia of certain dipterous, lepidopterous and other insects (Harvey, Cioffi & Wolfersberger, 1981, 1983; Harvey, Cioffi, Dow & Wolfersberger, 1983). Salivary glands (House, 1980), midgut (Wolfersberger, Harvey & Cioffi, 1982), Malpighian tubules (Maddrell, 1980), and rectum (Thurm & Küppers, 1980; Phillips, 1980) in many insects transport massive amounts of K^+ from basal to apical sides. This K^+ transport is used for ion regulation and fluid secretion. A K^+ pump in the epithelium of sensory sensilla in representatives of all orders of insects appears to be identical with that in these alimentary tissues (Thurm & Küppers, 1980). In sensilla the K^+ pump plays a key role in the generation of receptor potentials. In these important cases then, both osmotic and nervous functions in insects are coupled not to the Na^+,K^+ pump but to this unusual K^+ pump (Type V pump; Keynes, 1969). Unlike the Na^+, K^+ pump this K^+ pump moves K^+ out of cells; it is located on the apical rather than the basolateral plasma membrane; and it is not inhibited by ouabain (Harvey, Cioffi, Dow & Wolfersberger, 1983). However, K^+ transport is potently inhibited by a commercially important (and environmentally safe) insecticide, the delta-endotoxin from *Bacillus thuringiensis*. The selective toxicity of this agent may result from the presence of the Type V pump only in certain insect tissues. It may even be a chemiosmotic pump because it depends from moment to moment upon the oxidative metabolism; it is strongly electrogenic; its efficiency approaches 100%; and it appears to reside in 10 nm particles, portasomes, which resemble the mitochondrial F_1–F_0 ATPase (Harvey et al., 1981, 1983). A K^+ modulated ATPase has been identified and partially purified in pump-containing plasma membrane fractions of lepidopteran midgut (Wolfersberger et al., 1982) and dipteran sensilli (Wieczorek, 1982).

Current understanding of the physiology and cytology of the K^+ pump in insects is based on the study of the relatively small salivary glands, Malpighian tubules, rectum and sensory sensilla as well as the relatively enormous lepidopteran midgut (1–2 grams). However, for biophysical maneuvers such as short circuiting and flux measure-

† *Present address:* Department of Zoology, University of Cambridge, Cambridge, CB2 3EJ, U.K.

ments, and for biochemical isolation of specific regions of the epithelial cell plasma membranes, the large size of the midgut is an obvious advantage. For this reason, the isolated midgut of some lepidopteran larvae has been a favorite object for studying the mechanisms of K^+ transport during the past two decades. The localization of portasomes and of K^+ ATPase activity argue that the apical membrane of the so-called goblet cells, which borders a conspicuous apical cavity, is the site of the K^+ pump in midgut. Efforts to confirm this location by microelectrode and tracer kinetic pool studies have left unresolved questions. In 1978, Gupta, Berridge, Hall and Moreton investigated the location of ionic gradients in *Calliphora* salivary glands which secrete isotonic KCl. In addition to ion-selective microelectrodes they used their newly developed methods for the electron probe X-ray microanalysis (XMA) of elemental concentrations in frozen-hydrated cryosections (Gupta, 1976; Gupta & Hall, 1979, 1981). Gupta et al. (1978) found a clear concentration increment of K between the cytoplasm and the apical canaliculus establishing the location of the K^+ pump on the apical membrane in *Calliphora* salivary gland. In the present paper the methods of Gupta and Hall for XMA of cryosections have been applied to the posterior midgut of *Manduca sexta* larvae, where the goblet cells have a geometry similar to the secretory cells of *Calliphora* salivary glands. Not only is the route of K^+ transport greatly clarified but the results provide new insight into the function of the goblet cavity and into the biological functions of the K^+ pump.

Materials and Methods

Experimental Animals

Regular air-mail shipments of second instar larvae of the tobacco hornworm *Manduca sexta* were obtained from the Carolina Biological Supply Company. These insects were maintained on an artificial diet (supplied with the larvae), at 25° C, ambient humidity and a 16:8 hr light-dark cycle. Occasionally some larvae maintained similarly in the Zoology Department Culture at Cambridge were used. Experimental animals were fifth instar larvae of either sex, weighing 4.5 to 7 g. Larvae weighing 5 to 6 g were preferred because they are in a stable developmental period between the 4th larval moult and the larval-pupal moult; midguts from such larvae produced the most consistent performance *in vitro*. In most cases, the larvae were chilled in melting ice for 20 to 60 min before the dissection.

Collection of Blood and Gut Contents

The chilled larvae were tied at their heads and tails and stretched across a Petri dish. Blood was collected by micropuncture from one of the prolegs. The gut was exposed by a median dorsal incision along the length of the cuticle. The surface of the gut was blotted dry and samples of fluid from the anterior, middle and posterior midgut were taken by micropuncture. For XMA, samples of either blood or gut contents from four larvae were pooled; small droplets (about 1 µl) were placed on copper pins in a humidity box (Gupta & Hall, 1982), and quench-frozen immediately (*see below*). For photometric determination of sodium and potassium, samples of blood or gut fluids were collected from individual insects. Aliquots of 2 µl from each sample were diluted in 2 ml of water (AnalaR grade: British Drug Houses, Poole, U.K.) and measured with an SP90A flame photometer (Pye-Unicam Ltd., Cambridge, U.K.). For chloride determinations, 10 µl aliquots were analyzed on an electrometric titration apparatus (Ramsay, Brown & Croghan, 1955). The pH of the fluid samples was measured directly with a pH-electrode against standard pH solutions.

Midgut Chamber with Rapidly Removable Aperture

Signs of decreased K^+ transport by the isolated *M. sexta* midgut can be detected within half a minute after oxygen removal from the bathing solutions (resistance changes, Blankemeyer, 1976; cytochromes and ATP levels, Mandel, Riddle & Storey, 1980). Redistribution of ions both within cells and in extracellular compartments would be expected within a correspondingly short time period (*see* Coles and Tsacopoulos, 1979). To minimize this type of complication, a new chamber was adapted from a novel design of Wolfersberger & Harvey (*personal communication*) in which the midgut is mounted on the aperture of a "lollipop" which can be removed rapidly from the chamber (Fig. 1). The chamber in other respects is like that designed by Wood and Moreton (1978), to accommodate the fragile, low resistance, lepidopteran midgut. The midgut carrying 'lollipop' can be inserted into the chamber in less than 20 sec. At the end of the electrophysiological measurements the 'lollipop' can be pulled out and immersed into the cryogen within 1 sec of being under a specific experimental state (e.g. short circuit). The electrical alignment of the system is not disturbed either during assembly or disassembly of the chamber, which retains all the provisions for the measurement of transepithelial potential (TEP) and short-circuit current (SCC), as well as for the stirring of both solutions on both sides of the tissue with gas-lift pumps (Wood & Moreton, 1978). Oxygen gas was used for stirring except where stated otherwise.

Solutions

For all the experiments *in vitro* both surfaces of the tissue were bathed with saline containing (in mM): K^+, 32; Cl^-, 36; Mg^{2+}, 1; Ca^{2+}, 1; TRIS-HCl 5; sucrose, 266; pH, 8.3; total 341 mOsm. It is based on the saline used previously (Harvey & Wolfersberger, 1979) but the amount of sucrose is increased from 166 to 266 mM. It was determined beforehand that in this saline the midgut tissue performed better *in vitro* and the rate of decay of SCC was slower than in the lower osmolar solution.

Tissue

The posterior midgut tissue was used for *in vivo* and *in vitro* studies as (i) it has the highest K^+-flux ratio of all the midgut regions in *Manduca sexta* (Cioffi & Harvey, 1981); (ii) goblet cells in this region are tall and the projections (microvilli) of goblet cell apical membrane (GCAM) do not contain mitochondria (Cioffi, 1979); and (iii) it is the region used for membrane fractionation by Cioffi and Wolfersberger (1983). The gut was excised from chilled larvae, the tissue was prepared as a flat

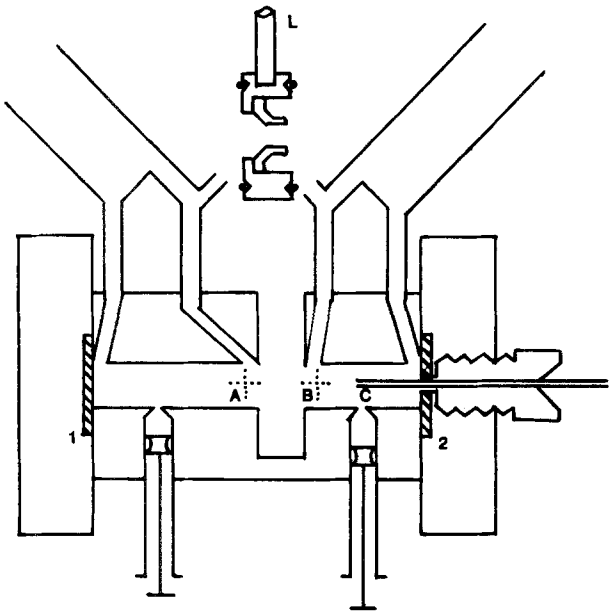

Fig. 1. Chamber used for *in vitro* experiments. The main chamber consists of an 8 mm diameter circular channel, with Ag/AgCl current electrodes (1,2) at either end. Three glass/agar bridges (*A, B, C*) are inserted into the chamber: the position of the right-hand electrode (*C*) is variable to allow precise alignment of the system. The tissue is mounted on an 8 mm ID aperture in a lollipop (*L*), which is then inserted into a groove in the main chamber, isolating the two halves. (Tests of the integrity of the seal showed that the inter-chamber resistance through the seal was at least 200 × greater than that through the tissue.) Saline is then added symmetrically to the two side arms until the fluid level is above the gas-lift pumps: saline then circulates independently in the two compartments. Drainage plugs allow for cleaning after an experiment

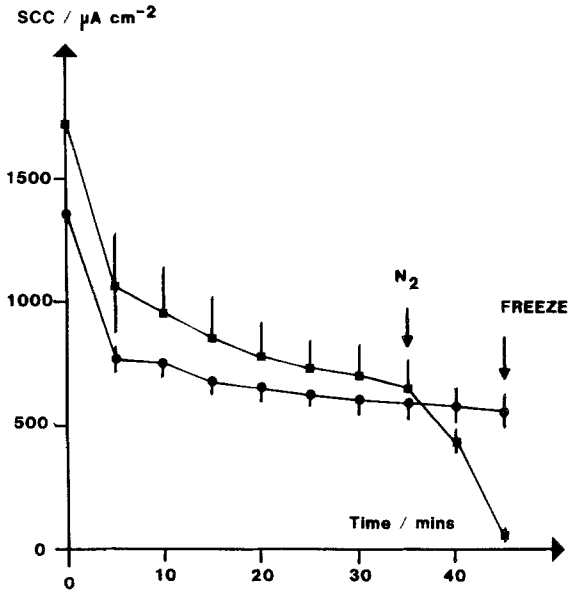

Fig. 2. The SCC of the five animals in the "short-circuit" oxygen group (●), and the four in the "anoxic" group (■), used for XMA. Data as mean ± SE: error bars are not shown where they would overlap. Nitrogen was supplied to the gas-lift pumps in the anoxic group at 35 min (arrow): both groups were quenched at 45 min

sheet (Harvey & Wolfersberger, 1979) and mounted on the 'lollipop' (Fig. 1). The preparation was checked for leaks, rinsed with oxygenated saline and carefully inserted into the chamber, which had been filled previously with oxygenated saline.

Electrical Measurements

To ensure that the physiological viability and the transport functions of every tissue sample were normal until within 1 sec of quench-freezing, complete records of electrical parameters were maintained by using methods previously described (Wood & Moreton, 1978; Harvey & Wolfersberger, 1979). These records are summarized below.

Short Circuit

After insertion of a piece of tissue into the chamber, an initial TEP of 60 to 120 mV (lumen side positive) was observed. The tissue was allowed to recover to a TEP of at least 100 mV, then short circuited with a voltage clamp (Wood & Moreton, 1978) for 45 min. This equilibration interval is longer than the period of rapid initial decay of SCC but is short enough for the K^+ transport to remain vigorous (Cioffi & Harvey, 1981). For anoxia experiments (to block active K^+ transport) the tissue was maintained under short-circuit conditions with oxygen gas for 35 min and then the gas lift pumps were switched to pure nitrogen gas ('White spot' grade – British Oxygen company, U.K.) for 10 min before quench freezing.

The records of SCC for both the oxygenated and the anoxic tissue samples are shown in Fig. 2. The two groups did not differ significantly until N_2 was applied to the anoxic group, whereupon the SCC fell rapidly (with an initial lag of 2.2 min while oxygen was exhausted from the bathing solutions) to about 10% of the SCC value in the control groups at 45 min. In the control experiments the mean value of SCC for the tissue at freezing was 552 ± 72 μA cm^{-2} ($n = 5$). Previously reported values (μA cm^{-2}) for SCC in lepidopteran midgut tissue after 45 min *in vitro* are: for *Manduca sexta,* 1300 (Cioffi & Harvey, 1981), 834 ± 65 ($n = 10$) (J.A.T. Dow, *personal communication*) and 327 (Moffett, 1979); for *Antheraea pernyi,* 706 (Wood, 1972); for *H. cecropia,* 770 (Wood & Moreton, 1978); and for *P. cynthia,* 160 (Giordana & Sacchi, 1977). The tissue samples used for XMA were therefore actively transporting K^+ at a high level to within 1 sec of quench freezing.

Open-circuit

The gut tissue was maintained under open circuit in the presence of oxygen gas throughout 45 min before quench-freezing. The mean TEP recorded from the four animals used under this regime is plotted in Fig. 3. The TEP increased steadily over the first 10 min to a maximum of 106 mV and then slowly declined to 80 ± 2 mV at 45 min. Comparable published values for open-circuit TEPs at 45 min are: 70 mV for *Manduca sexta* (Moffett, 1979); 78 mV for *P. cynthia,* 51 mV for *Macrothylatia rubi,* and 48 mV for *Bombyx mori,* all obtained by Giordana and Sacchi (1977).

Control Tissue *in Vivo*

For comparisons with tissue samples *in vitro,* posterior midgut tissue was also quench frozen quickly after excision without exposure to any saline. The guts were removed as described above except that for these experiments the larvae were not

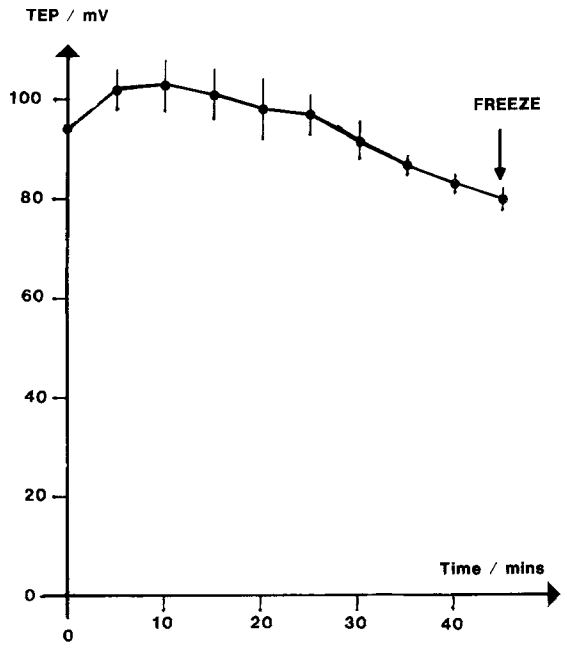

Fig. 3. The TEP developed by the four experimental animals in the "open circuit" group used for XMA. Values are presented as mean ± SE (apical side positive), as are all data in this paper. The tissue was quench-frozen at 45 min

chilled. The massive gut contents still enclosed in the peritrophic membrane were gently pulled out and the posterior midgut tissue was quench-frozen by plunging it into the cryogen.

Cryopreparation

Supercooled Freon 13 (monochlorotrifluoromethane, m.p. −181 °C) was used to quench-freeze the tissue and body-fluid samples. The cryogen was supercooled by vigorous stirring in a 100 ml plastic beaker filled to the brim with Freon and immersed in liquid nitrogen (Somlyo & Silcox, 1979). Suitable precautions were taken to avoid the formation of frost within the beaker and of a layer of cold gas above the cryogen surface. The temperature of Freon was continuously monitored with a thermocouple placed in the upper layer of the fluid and was in the range of −185 to −190 °C at the moment of specimen immersion.

Copper pins bearing fluid droplets were frozen using a quenching machine (Barnard, 1982; Gupta & Hall, 1982). Lollipops bearing the gut tissue were withdrawn from the midgut chamber, given a sharp jerk to shake off extra fluid and rapidly thrust into the stirring cryogen by hand. The frozen samples were removed from the cryogen, shaken free of excess Freon and immediately transferred to liquid nitrogen for further handling and storage at −196 °C. For *in vitro* samples, only pieces of the gut tissue from the center of the aperture in the lollipops were pushed out under liquid nitrogen and used for cryosectioning when required. It should be noted that apart from the sucrose no Dextran or any other 'cryoprotectant' was added to the bath saline.

Frozen-hydrated blocks of either fluid droplets on pins or suitable pieces of frozen tissue clamped into a brass chuck in a pocket of indium metal were cryosectioned at temperatures between −65° and −75 °C, using steel knives and a large cryostatmicrotome (SLEE, London, U.K.). 1 to 2 μm thick frozen-hydrated sections were transferred to carbon-coated nylon films stretched over multislot nickel grids (Polaron, 60/62 Greenhill Crescent, Watford, Herts, U.K.) mounted on nickel holders. Section-bearing holders were transferred from the cryomicrotome to a liquid nitrogen Dewar for storage at −190 °C until required for microanalysis. Details of these operations can be found elsewhere (Gupta, Hall & Moreton, 1977; Gupta & Hall, 1979, 1981, 1982).

Electron Probe X-ray Microanalysis

The cryosections were analyzed in a JEOL JXA-50A electron probe microanalyzer (JEOL Ltd., Tokyo, Japan) operated at 45 kV, and fitted with a liquid nitrogen-cooled transmission stage (−170 °C) protected by an anticontamination shield (−190 °C). X-ray spectra were collected with a Kevex-Link energy dispersive Si(Li) spectrometer (horizontal specimen, take-off angle 35°, distance 20 mm, detector area 30 mm^2, resolution 155 eV FWHM), using a beam current of 1.0 nA over 100 sec lifetime. Both the beam voltage and current were continuously monitored throughout every run. To keep a close check on the loss of mass from the specimen field under the beam, the continuum X-ray counts (4.5 to 18 keV) were also continuously monitored for each run and the image profile was watched on a video display wave form monitor (Hall & Gupta, 1982*a*).

The deconvolution of the X-ray energy spectra and the data reduction to obtain values of elemental concentration in mmol/kg were carried out with an on-line computer and the Link Systems QUANTEM/FLS software program. The program uses a continuum normalization procedure (Hall, 1971) and includes a standards file, G-factor iteration, mass thickness standard, absorption corrections for characteristic X-rays and a comprehensive subtraction from the continuum of background X-rays generated by the substrate film and other extraneous sources (grid holder, etc).

All cryosections were analyzed first in the hydrated state to obtain elemental concentrations (in mmol/kg wet mass). The sections were then dried within the microanalyzer and reanalyzed to obtain data in mmol/kg dry mass. The two sets of data were then used to estimate the dry mass fractions (f_D) and tissue H_2O in every analyzed compartment (Gupta et al., 1977; Gupta & Hall, 1979). A specimen was judged fully hydrated from: (a) the low contrast and a lack of visible detail in the scanning transmission image; (b) the comparison of concentration values with the known values of K and Cl in the saline, and (c) by comparing the concentration values obtained by two different methods of X-ray data reduction viz. the 'continuum method (C−N)' and the 'characteristic counts alone (C−A)' method (*see* Hall & Gupta, 1982*b*, for further details). In cases where significant mass loss was suspected, the values (in mmol/kg wet mass) obtained by the C−A method were preferred. Final collation of data was executed on an IBM 3801 computer using programs written under the Statistical Analysis System package. Formulations and further details of quantification procedures can be found in a number of previous papers (Gupta & Hall, 1979; Hall & Gupta, 1979, 1982*b*).

In this study 7 elements (Na, Mg, P, S, Cl, K and Ca) were measured simultaneously in each of 658 sites analyzed in 213 cells from the posterior midguts of 26 larvae.

Results

Identification of Analyzed Sites

Although the *M. sexta* midgut epithelium is known to be composed of a single layer of cells (Cioffi,

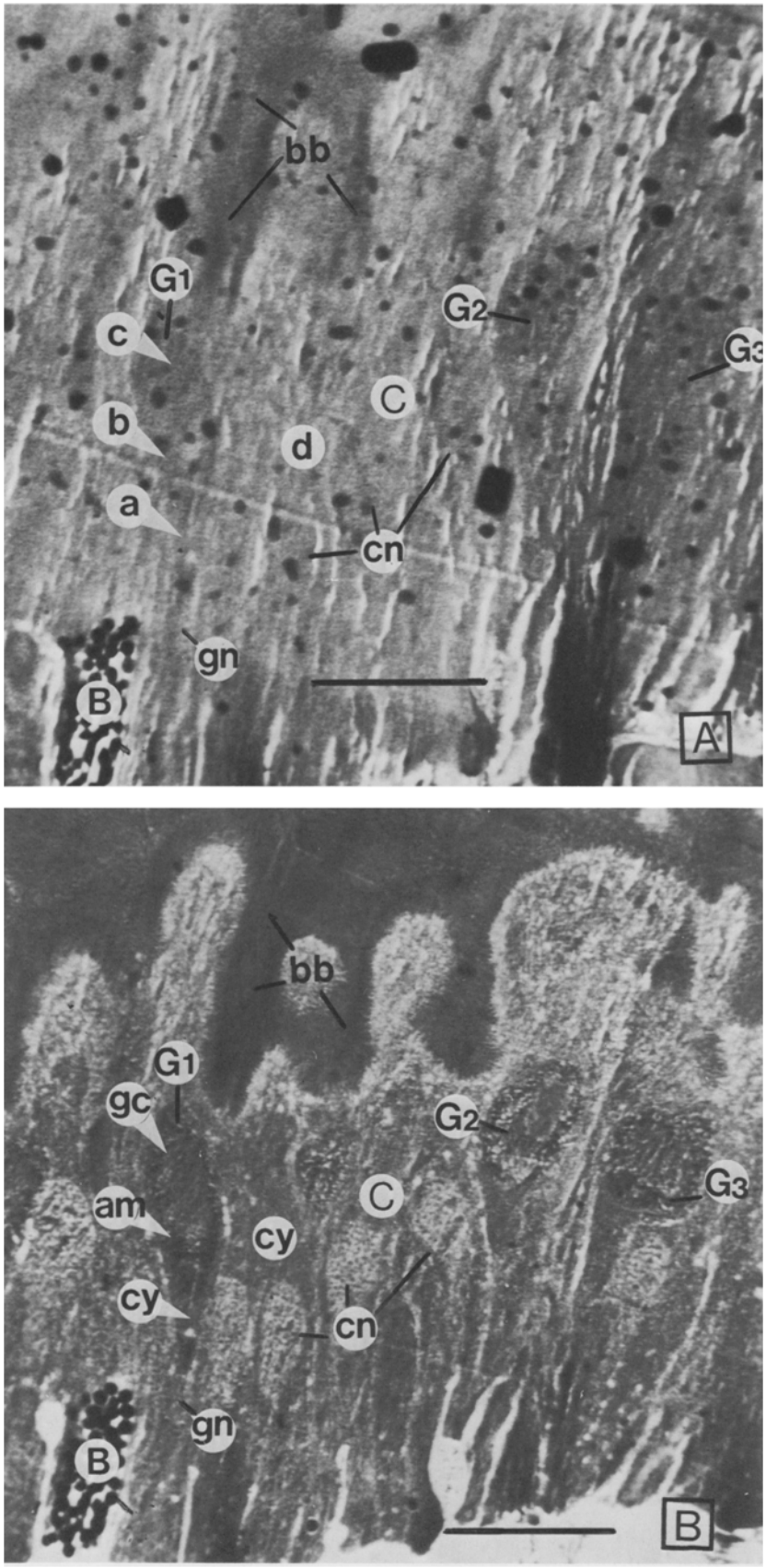

Fig. 4. Scanning transmission electron micrographs in bright-field/dark-field mode from 1 μm thick cryosections of the midgut tissue from short-circuited sample. Image from a fully hydrated section (*A*) is compared with the image from an adjacent frozen-dried section mounted separately. Dense granules scattered over the micrograph represent coarse frost inevitably present on frozen-hydrated sections. *am* = apical membrane folds; *B* = basal regenerative cell; *bb* = brush border of columnar cells; *C* = columnar cells; *cn* = columnar cell nuclei; *cy* = cytoplasm; *G1-G3*, goblet cells; *gc* = goblet cavity; *gn* = goblet cell nucleus. Scale bar = 10 μm. Arrowed spots *a, b, c* and *d* indicate subfields from which X-ray energy spectra *A, B, C* and *D* in Fig. 5 were collected at a higher magnification

1979), the presence of circular and longitudinal muscles on the basal surface throws the epithelium into a complex series of folds and crypts. Therefore, the total thickness of the tissue in frozen blocks is often 0.5 mm or more. In any single section the epithelial cells are cut in all possible directions with respect to their normal basal-apical axes and the crypts are usually packed with a dense mat of columnar cell microvilli (e.g., Fig. 4*B*), with little apical free space. Furthermore, the scanning transmission images (STEM) of 1 μm thick fully hydrated cryosections have characteristically low differential contrast (Fig. 4*A*) which is, however, immensely improved after dehydration (Fig. 4*B* and 6). Thus to identify tissue areas of interest it was found helpful first to examine a dehydrated section and record the STEM images from the most suitable fields and then to analyze other holders bearing hydrated sections in the same series from the same block. In addition the mineralized "spherites" found in basal regenerative cells (Turbeck, 1974) had conspicuously high electron density even in fully hydrated sections (*B* in Fig. 4) and provided a marker for the basal side, while the smooth mat of columnar cell microvilli defined the apical side (*bb*, Fig. 4). It therefore proved possible to identify and analyze all the major tissue compartments even in frozen-hydrated sections.

As an example, Fig. 4*A* is a STEM image from a hydrated (>95%) field of the tissue section from a short-circuit regime, whereas Fig. 4*B* is from an adjacent section fully dehydrated on another holder. All the cell types and the major subcellular compartments can be clearly recognized in Fig. 4*B* but can also be made out, albeit faintly, in Fig. 4*A*. Further confirmation that the analyzed fields were clearly resolved is illustrated by some representative X-ray energy spectra (Fig. 5) collected at a higher magnification and using rasters of about 1 μm^2. The spectrum 5*A* is from the apical cytoplasm (*a* in Fig. 4*A*) of the goblet cell (GC1); 5*B* is from the GCAM projections (*b* in Fig. 4*A*); and 5*C* is from the goblet cavity (*c* in Fig. 4*A*). The high phosphorus signal from the goblet cell cytoplasm (Fig. 5*A*) is absent from the goblet cell cavity (Fig. 5*C*). The area representing GCAM (Fig. 5*B*) includes cytoplasmic projections as well as the extracellular space (ECS) between them because individual projections cannot be resolved in our analytical system. Here the intermediate level of phosphorus represents the cytoplasmic component (projections or microvilli) while slightly elevated sulfur, chloride and potassium peaks are indicative of the extracellular component. Since the ECS in such fields is the immediate space into

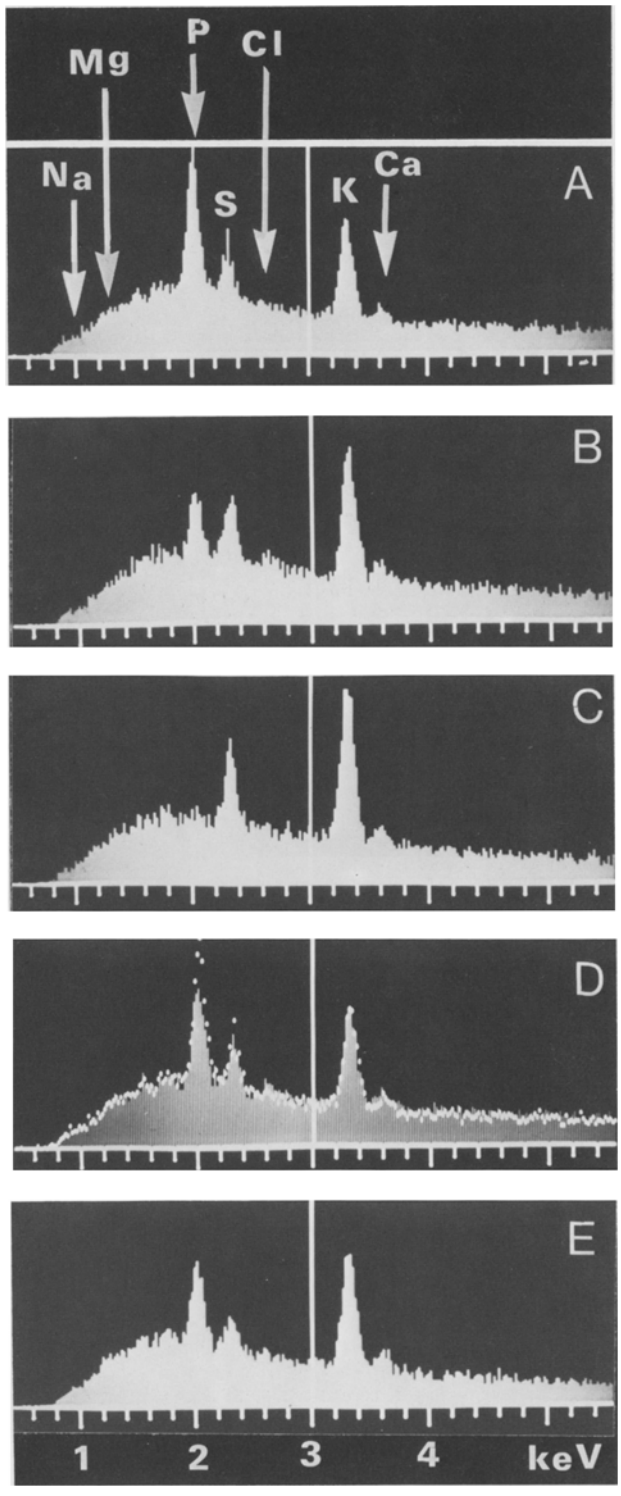

Fig. 5. X-ray energy spectra from a 1 μm thick frozen-hydrated section (*cf.* Fig. 4*A*). *A*, goblet cell apical cytoplasm; *B*, goblet cell apical membrane folds; *C*, goblet cavity; *D*, columnar cell apical cytoplasm (bars) compared with spectrum *A* (dots); *E*, muscle cell. The peaks labeled *Ca* include contributions of X-ray quanta from potassium K_β radiation which are removed during computer deconvolution for the final estimation of calcium

which the putative K^+ pumps on GCAM are directed, a knowledge of K concentration here is of considerable interest. Although the narrow spaces are not directly resolved, the phosphorus levels in such 'average' spectra (Fig. 4*B*) can be used to estimate the cytoplasmic volume fraction in the analyzed subfields and to estimate better the true elemental composition in the ECS by using simultaneous equations on the assumption that the intracellular elemental concentrations in the field are identical with those in the apical cytoplasm (Gupta et al., 1978). Such estimated values have been used in Figs 7 and 8 both for GCAM and for the columnar cell brush border.

Figure 5*D* compares X-ray energy spectra, from the goblet cell cytoplasm (dots), and from the columnar cell cytoplasm (bars) (*d* in Fig. 4*A*). The levels of the X-ray continuum background and the heights of the K-peak are the same in both sites; but the phosphorus and sulfur peaks are higher in the goblet cell cytoplasm, presumably due to a high concentration of mitochondria in this region (Cioffi, 1979). It should be emphasized that in our microanalytical system it is not usually possible to resolve individual cytoplasmic organelles unless they are larger than 1 μm. The analyses from cytoplasm in this report therefore do not refer to the cytosol alone but include signals from organelles such as mitochondria, endoplasmic reticulum, etc. A spectrum from a muscle cell (Fig. 5*E*) is included for comparison.

Figure 5*A–C* also reveals qualitatively a stepwise increase in the K peaks from the apical cytoplasm through to the goblet cavity. In fact, out of the five subcompartments of the short-circuited tissue represented by these spectra, the K peak is highest in the goblet cavity (Fig. 5*C*). The X-ray continuum levels are the same in all these spectra (thus indicating more or less the same local mass thickness); the qualitative differences in characteristic peak heights therefore represent truly quantitative differences in the elemental concentrations in these fields.

Figure 6 illustrates the quality of structural preservation which was achieved in the cryosections from the tissue blocks prepared under different experimental regimes.

Quantitative Data

The elemental concentrations (in mmol/kg wet mass) in all the major compartments of the posterior midgut tissue in four steady-state conditions of transport are summarized in Tables 1 and 2. The last column in these Tables lists the local dry weight fractions (f_D) for each site. The data for Na are not included in these Tables because the Na values obtained by energy dispersive spectrometry (EDS) were not found to be significantly above zero (Students *t*-test, one-tailed) at any site in the tissue sections. This is not surprising for the tissue *in vitro* because no Na was included in the bath saline. However, the larval blood is known to have about 15 mM of Na (*see* Table 3) and therefore one might expect some Na in the cells *in vivo*. Since the minimum measurable concentration of Na with EDS is about 20 mmol/kg local mass (Hall & Gupta, 1982*a*), the absence of detectable Na in the cells in EDS results was confirmed from time to time by using a wavelength dispersive X-ray spectrometer (WDS) available on our microanalyzer. WDS can measure Na down to 5 mmol/kg wet mass even in a hydrated section (Hall & Gupta, 1982*a*). In practice, no detectable Na was found in any epithelial cell even in the fresh (*in vivo*) gut samples, thus confirming that under normal conditions Na^+ transport in this tissue is not significant (Harvey & Nedergaard, 1964; for reviews *see* Harvey, 1982; Wolfersberger et al., 1982). Similarly the EDS measurements for Ca in our data are also subject to a larger error than for the other elements (Gupta & Hall, 1978).

The general levels of the five other elements analyzed in all the subcompartments within goblet and columnar cells are the same under three conditions of K transport. These levels are also in line with the published XMA data from a number of transporting epithelia from other animals (Gupta & Hall, 1979, 1982). For this tissue the most notable features of the data are that: firstly, the K levels in the goblet cells are not very different from those in the columnar cells either *in vivo* (Table 2B) or *in vitro* (Tables 1A and 2A). Secondly, the highest levels of K are found in the goblet cavity: surprisingly these levels are the same for the tissue *in vivo* (163 ± 11 mmol/kg wet mass) and under short circuit *in vitro* (158 ± 4 mmol/kg wet mass). Thirdly, the average K levels at the GCAM border are somewhat higher than in the supranuclear cytoplasm (it was not found possible to measure the narrow basal cytoplasmic foot of the goblet cells). Finally, after anoxia (Table 1B) which abolishes SCC by inhibiting K^+ transport, the major changes in ionic distribution are decreases in K concentration by 40 mM in goblet cytoplasm, by 70 mM in GCAM border and by 100 mM in goblet cavity. These changes are precisely those predicted if the goblet cell apical membrane is the site of the K^+ pump.

Expressing the XMA data in mmol/kg wet mass is likely to mask the true levels of free K^+

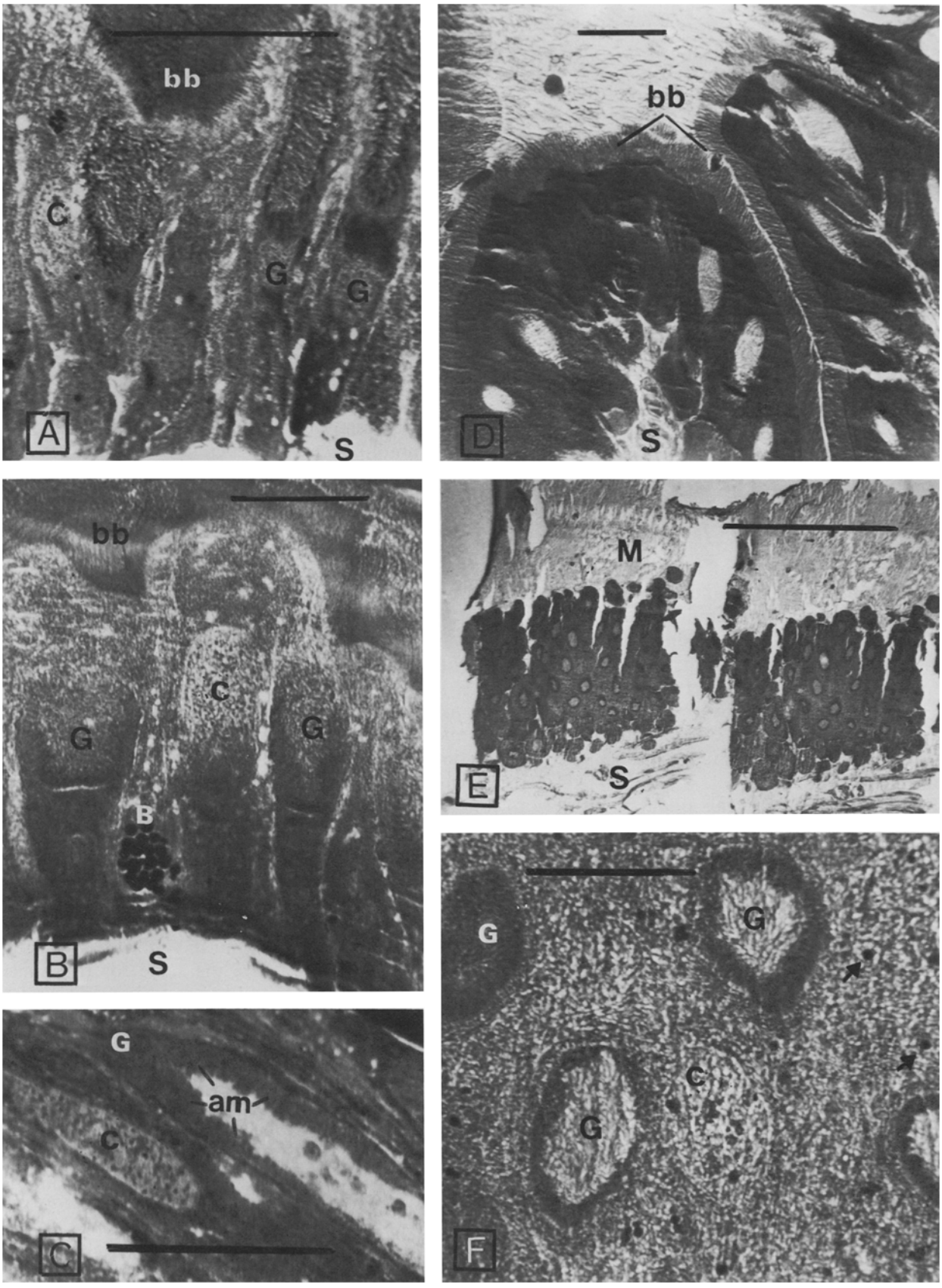

Fig. 6. Some representative STEM images under bright-field/dark-field modes from 1 to 2 μm thick frozen-dried cryosections: *A*, from a short-circuited sample, *S* is serosal tissue. *B*, from an open-circuit sample. *C*, another field from a short-circuited sample to show the details of the goblet cell apical folds (*am*). *D*, from an anoxic sample; note details of the columnar cell brush border. *E*, from tissue-block frozen immediately after excision (*in vivo*). *M*, mucosal (apical) side (food), *S*, serosal (basal) blood. *F*, a small field from *E* at a higher magnification. Scale bars represent 10 μm except in *E* where the bar is 100 μm. Labeling as in Fig. 4

Table 1. Elemental concentrations[a] and % dry wt. ($f_D \times 100$) in the posterior midgut of *Manduca sexta* larvae under short circuit with oxygen (A) and under anoxia (B). (All values are mean ± SE[b])

Probe site	*n*	Mg	P	S	Cl	K	Ca	$f_D \times 100$
				mmol/(kg wet mass)				
(A) With Oxygen								
Medium:								
Serosal	17	(1±1)	(2±2)	4±2	29±4	27±4	1±0.4	7±1
Mucosal	15	(2±4)	(11±6)	9±3	31±3	43±6	(1±1)	8±1
Goblet Cells:								
Nucleus	9	14±2	205±13	56±4	12±2	134±7	(2±2)	27±2
Cytoplasm	22	12±2	189±16	61±5	21±3	130±5	(0±2)	30±3
GCAM-border	23	8±1	131±13	82±9	24±4	146±12	(−1±1)	29±3
Gob. cavity	25	(−1±2)	10±2	58±7	31±5	158±4	(−2±2)	21±3
Columnar Cells								
Nucleus	4	14±4	220±43	50±8	16±4	146±12	(−0.3 ±0.5)	23±2
Cytoplasm	20	17±3	168±16	51±4	12±2	129±7	4±1	27±3
Brush border	14	5±2	110±17	65±8	19±4	96±7	2±1	24±2
(B) Anoxia (N_2)								
Medium:								
Serosal	5	(1±2)	(1±2)	(2±2)	29±2	31±1	2±0.5	6±1
Mucosal	8	(1±1)	(2±1)	(2±1)	34±5	38±5	(1±1)	6±1
Goblet Cells:								
Nucleus	7	17±2	240±36	73±10	20±3	123±14	(2±1)	34±3
Cytoplasm	11	14±2	164±18	56±8	16±2	91±7	4±2	30±3
GCAM border	24	10±1	80±9	46±7	19±2	78±6	4±1	24±2
Gob. cavity	30	4±1	9±2	16±2	15±2	61±4	4±1	10±2
Columnar Cells:								
Nucleus	6	16±2	227±6	60±3	13±2	132±4	3±1	24±1
Cytoplasm	23	21±2	216±20	77±5	19±2	127±4	7±2	31±2
Brush border	18	14±2	90±5	62±6	27±4	98±4	1±0.4	21±2

[a] Na values are not included because Na levels were not found significantly above zero at any site.
[b] Values in parentheses indicate that these are not significantly greater than zero ($P=0.05$), Student's *t*-test, one-tailed).

in cell water because of local variations in the dry mass fractions (f_D). Although, such values cannot be measured directly with the XMA, an estimate of total K concentration in mmol/kg local H_2O can be obtained by dividing the values in Tables 1–3 by $(1-f_D)$. Such a conversion is valid because $(1-f_D)$ provides the most direct estimate of the local water fractions; but such a conversion assumes that all the local water fraction is solvent and all the measured K is free. For a similar K^+-transporting system, the salivary gland of *Calliphora*, this assumption has been validated by parallel measurements of K^+ and Cl^- with ion-selective microelectrodes (Gupta et al., 1978). Calculated values for average epithelial K concentrations and water content are shown in Table 4. Control midguts, whose water content was measured by wet/dry weighings after 45 min under open circuit in an identical saline, were found to contain 72±1% water ($n=10$). We have converted the K data into mmol/kg H_2O and plotted it in Fig. 7 and 8. Furthermore, as mentioned before, in these plots the K value for the GCAM border is the estimated 'real' value for the extracellular fraction. It is clear from these Figures that the major uphill step for K^+ out of the cells is at the GCAM, especially in SCC and *in vivo* samples.

The highest K gradient across the GCAM in Fig. 7 is obtained from the tissue *in vivo*. The tissue in freshly excised midguts was much more folded and most of the data had to be collected from tangentially cut cells (Fig. 6*F*). The tangential sectioning proved an advantage for measuring K at the cytoplasmic side of GCAM without interference from the large aggregate of mitochondria (Fig. 6*B*) in the supranuclear cytoplasm (Cioffi, 1979); hence the cytoplasmic values from these sites in the *in vivo* samples are more likely to represent the ionic levels within the apical folds, which are also free from mitochondria. Similar measurements from *in vitro* samples proved impossible because the medium with 266 mmol sucrose is some-

Table 2. Elemental concentration[a] and % dry wt. ($f_D \times 100$) in the posterior midgut of *Manduca sexta* larvae under open circuit (A) and *in vivo* (B). (All values are mean ± SE[b])

Probe site	*n*	Mg	P	S	Cl	K	Ca	$f_D \times 100$
		mmol/(kg wet mass)						
(A) Open Circuit:								
Goblet Cells								
Nucleus	8	14±1	192±23	45±2	11±1	97±13	(0)	29±3
Cytoplasm	19	18±3	174±17	51±3	12±2	108±11	2±1	32±3
GCAM-border	18	11±1	110±10	55±5	13±1	118±6	3±1	27±2
Goblet cavity	9	2±1	14±2	59±5	19±2	124±9	2±1	24±2
Columnar Cells								
Nucleus	4	16±2	178±12	38±4	9±1	101±11	(2±1)	25±2
Cytoplasm	16	23±2	198±8	51±4	12±1	118±8	(2±2)	35±3
Brush border	11	10±2	94±7	58±11	27±2	109±9	3±1	29±3
(B) *In Vivo:*								
Blood	11	18±3	34±3	10±1	22±2	36±4	5±1	5±0.2
Goblet Cells								
Nucleus	8	14±3	147±21	43±5	13±1	113±14	2±1	19±1
Cytoplasm	14	11±2	133±11	42±4	15±1	94±7	1±0.5	18±1
GCAM-border	11	3±1	82±7	53±3	18±3	126±14	2±0.7	21±1
Goblet cavity	16	2±1	21±2	31±2	28±2	163±11	(−1±0.7)	14±1
Columnar Cells								
Nucleus	4	11±2	85±14	36±3	10±1	123±13	(1±1)	16±1
Cytoplasm	8	17±3	133±8	39±3	11±1	104±4	1.5±0.2	17±1
Brush border	10	21±3	65±10	20±3	33±6	95±7	4±1	8±0.5

[a] Na values are not included because Na levels were not found significantly above zero at any site.
[b] Values in parentheses indicate that these are not significantly greater than zero ($P = 0.05$, Student's *t*-test, one-tailed).

Table 3. Comparison of blood and gut contents of fifth instar *Manduca sexta* larvae

Region	Method[a]	*n*	Elemental Concentrations mmol/(kg wet weight)														pH		
			Na		Mg		P		S		Cl		K		Ca				
			mean	SE	mean	SE	mean	SE	mean	SE	mean	SE	mean	SE	mean	SE	mean	SE	*n*
Blood (whole)	XMA	10	17	4	30	7	48	7	8	2	29	3	25	3	8	2			
	PHOT(1)	10	14	2	38	3							22	2	12	3			
	PHOT(2)	5	5	1							27	2	26	2			6.7	0.06	6
Anterior midgut	XMA	8	(−18	5)	(−1	2)	18	3	17	3	8	2	207	20	(0	0.8)			
	PHOT(2)	4	1	0.4							8	0.6	179	23			10.4	0.2	4
Whole midgut fluid	PHOT(1)	8	3	0.6	4	2							157	16	10	3			
Posterior midgut fluid	XMA	9	(−28	4)	(0.8	2)	19	2	12	1	27	2	142	12	1	0.5			
	PHOT(2)	4	1	0.3							18	2	210	12			9.6	0.2	4
Food	PHOT(2)	3	21	5							24	5	70	9			5.0	0.01	9

[a] XMA: XMA of Carolina larvae, July 1982. Analyses were performed on single samples, pooled from 4 larvae: *n* represents the number of determinations made on each sample. PHOT(1): Emission flame photometry of samples from Cambridge larvae, June 1981 (J.A.T. Dow & J.H. Spring, *unpublished observations*). Each measurement was made on fluid from a single animal; *n* represents the number of animals in each group. PHOT(2): Emission flame photometry, chloride titration and pH electrode determinations of Carolina larvae, August 1982. Each measurement was made on fluid from a single animal; *n* represents the number of animals in each group.

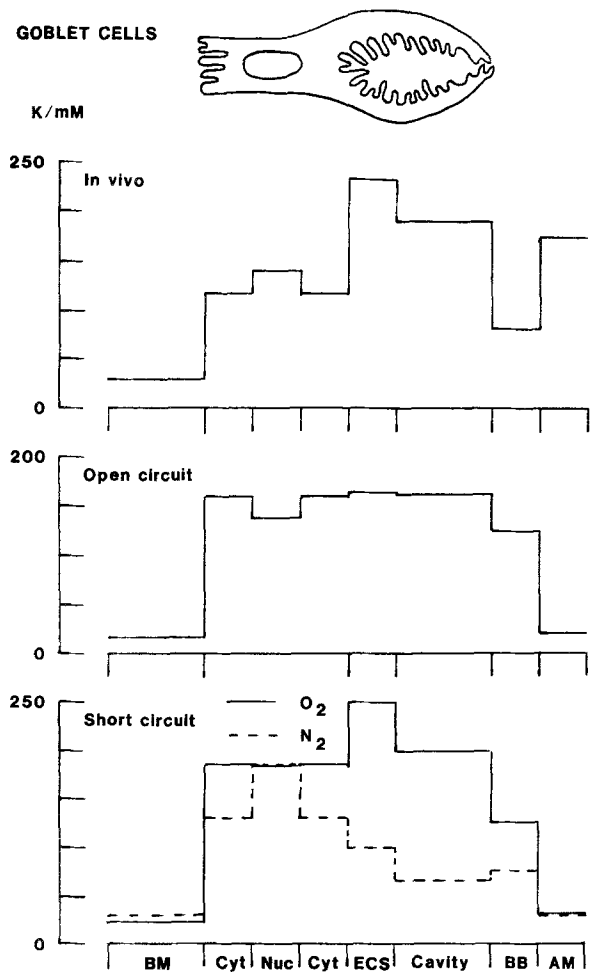

Fig. 7. Distribution of K (in mmol/liter local water) in the goblet cells under four steady-state conditions of transport. *BM* = basal medium; *Cyt* = cytoplasm; *Nuc* = nucleus; *ECS* = calculated extracellular space concentration for microvillar field; *BB* = columnar cell brush border (calculated *ECS* concentration); *AM* = apical medium

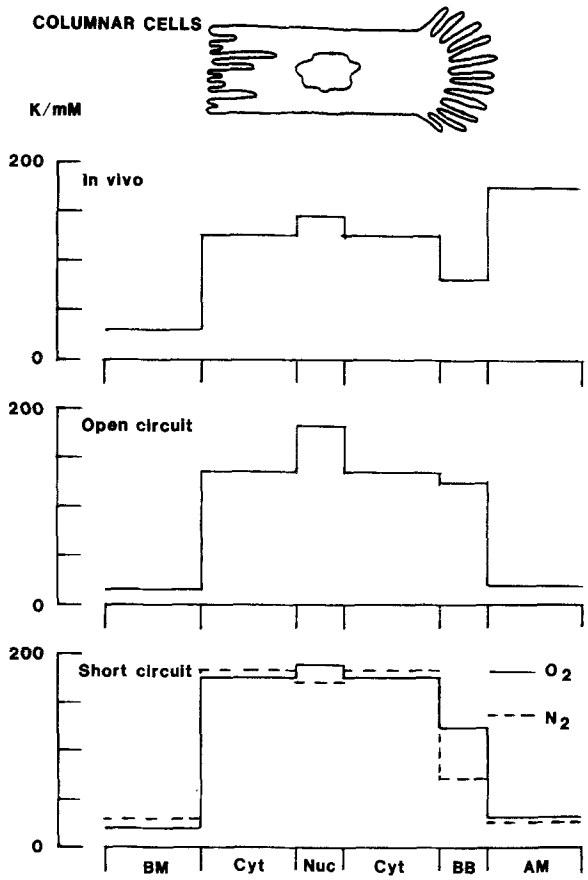

Fig. 8. Distribution of K (mmol/liter local water) in columnar cells in four steady-state conditions of transport. Values in brush border are calculated values for the extracellular spaces. Abbreviations as for Fig. 7

what hypertonic and therefore causes appreciable shrinkage in the epithelial cell bodies (Moffett, 1979): This shrinkage is reflected in elevated values for P, S and f_D in all of the *in vitro* samples as compared to the values *in vivo*. For columnar cells the cytoplasmic values include measurements from the apical as well as basal sites, but most of the data were collected from the extensive supranuclear part of the cell. The basal cytoplasm forms rather narrow channels separated by deep basal membrane infolds (Cioffi, 1979). In general the K levels at these basal sites were lower, and both phosphorus and magnesium levels higher, than in the apical cytoplasmic sites of columnar cells. The elemental values for the columnar cell brush border in Tables 1 and 2 are, as for GCAM-border, the average values. The estimated real K levels in the narrow extracellular channels between long microvilli are given in Fig. 8.

Table 4. XMA estimates for the total epithelial cell K in *Manduca sexta* posterior midgut. (Basal regenerative cells and goblet cavities are not included in these estimates.)

Experimental conditions	Total sites	K mmol/kg wet wt	% water $(1-f_D) \times 100$	K mmol/kg water
			(Mean ± SE)	
In vivo	53	109 ± 6	82 ± 1	134 ± 7
In vitro:				
Open circuit	76	109 ± 9	71 ± 2	154 ± 13
Short circuit:				
Oxygen	92	130 ± 7	73 ± 3	178 ± 10
Nitrogen	89	108 ± 9	72 ± 2	150 ± 12

Mineralized Concretion Spherites

Most of the Mg and some of the P in epithelial cells in this tissue appears to be associated with

small dense granules found scattered to a variable extent in the cytoplasm (e.g. Fig. 6*F*, small arrowheads). When measured at high magnifications with static probes, these granules proved to be almost pure magnesium phosphate. Similar magnesium phosphate bodies are found as large spherites filling the cytoplasm of basal regenerative cells (Fig. 4*A* and *B*). These spherites in basal cells contained (mmol/kg wet mass) Na 50 ± 22; Mg 4384 ± 471; P 4512 ± 482; S -38 ± 13; Cl -5 ± 4; K 252 ± 12; Ca 60 ± 8; f_D 0.6 ($n=4$). In comparison the narrow strips of cytoplasm between the spherites in the basal cells contained: (Na -5 ± 4; Mg 40 ± 5; P 153 ± 18; S 31 ± 8; Cl 11 ± 3; K 121 ± 21; Ca (-1 ± 1); f_D 0.28 ($n=4$). Apart from demonstrating the analytical spatial resolution possible with the microprobe technique, these data show that the spherites are almost crystalline magnesium phosphate with small but significant amounts of Na, K and Ca. However, care was taken to exclude such granules as far as possible from the analyzed sites in goblet and columnar cells. It is possible that in chemical analyses of the tissue ions, most tissue Na has been from these spherites with none free in cells. These analyses are broadly similar to others for invertebrate concretion bodies, as recently reviewed by Brown (1982).

Muscle Cells

A few measurements of the tenuous muscle fibers in transverse profiles revealed (in mmol/kg wet mass): (Na 4 ± 8); Mg 14 ± 3; P 63 ± 8; S 33 ± 5; Cl 12 ± 4; K 100 ± 8; Ca 1.6 ± 1; f_D 0.15 ($n=4$). After anoxia the elemental concentrations were (Na 5 ± 10); Mg 9 ± 2; P 62 ± 3; S 35 ± 4; Cl 9 ± 1; K 105 ± 5; Ca 1.4 ± 1; f_D 0.14 ($n=5$). Thus, the muscle cells do not show any apparent change either in elemental composition or in f_D after 10 min of anoxic conditions. These concentrations in gut muscle cells are similar to those found by Somlyo, Somlyo and Shuman (1979) using XMA on ultrathin cryosections of rabbit vascular smooth muscle.

Analysis of Blood and Gut Contents

The concentration of elements (in mmol/kg wet mass) for the blood, and for the lumen contents from anterior, middle and posterior midgut are shown in Table 3. The results obtained by XMA of micropuncture samples are compared with the two sets of previous data from conventional chemical analyses. Wherever the comparable values are available the agreement between the two methods of analysis is excellent. The blood ion values are also similar to those found in the prepupae of *Manduca sexta* by Jungreis (1978). Na, Mg and Ca occur at significant levels in blood but are not detected in the gut contents. K is by far the dominant cation in the gut lumen, reaching a level of 5 to 10 times that in blood. Cl almost balances K in blood while (Na + Mg + Ca) approximates (P + S). It is likely that Na, Mg, P and S are not free but are associated with particulate inclusions commonly found in insect blood. The gut fluid contains only $^1/_5$ to $^1/_{20}$ the Cl concentration expected for a KCl solution, suggesting that the K^+ here is balanced by an undetermined anion.

The pH of blood is constant at 6.6. For gut contents the pH values in micropuncture samples are somewhat lower than the corresponding values obtained by directly inserting a pH electrode into the midgut, suggesting that the pH of gut contents is labile. The highest pH value has been recorded in the middle zone of the midgut (*see* Harvey, 1982). Since the processing of food occurs linearly from the anterior to the posterior midgut, it must be the corresponding midgut epithelium which maintains the high luminal pH characteristic of larval lepidoptera.

Discussion

Active K^+ secretion by the midgut of the lepidopteran larvae was established unequivocally by Harvey and Nedergaard in 1964. The present XMA study on hydrated and dried cryosections of *Manduca sexta* larval midgut provides fresh insight into three persisting questions. (A) What route is taken by the potassium ions as they are transported across the epithelium from basal to apical side? (B) What is the role of the cavity formed by the invagination of the particle-studded apical plasma membrane of the goblet cells into which the K^+ transport appears to be directed? (C) What is the biological function of the K^+ pump? Each of the three parts of the discussion attempts to answer one of these questions.

K^+ Transport Route

Types of Evidence for K^+ Pump on GCAM

Electron microscopy has revealed that particles characteristic of K^+-transporting insect cells are restricted to the goblet cell apical membrane. However, the hypothesis that the particles are the units of K^+ transport (Anderson & Harvey, 1966; Gupta & Berridge, 1966) i.e. that they are K^+

pumps or portasomes (Harvey, 1980; Harvey et al., 1981, 1983) remains unproven. Isolated plasma membrane fragments, containing GCAM, show K^+ ATPase activity (Wolfersberger et al., 1982), but this activity so far has not been proven to be localized exclusively in GCAM (Harvey et al., 1983). The present XMA data bear on a third type of evidence – that the K^+ electrochemical gradient is across the goblet cell apical membrane.

Tissue K Concentration

Previously the midgut tissue K concentration has been estimated at 90 to 140 mM (cell water) by conventional chemical methods (Harvey, Wood, Quatrale & Jungreis, 1975; Giordana & Sacchi, 1977; Zerahn, 1977). In such estimates it was not possible to distinguish between different epithelial cell types, let alone to identify subcellular compartments as is possible with XMA. For a comparison with the previous data the values for individual compartments in Tables 1 and 2 were converted into average values for cell K under each experimental condition (Table 4). The overall average value, 134 ± 7 mM K (cell water), is in excellent agreement with the estimate of 140 mM K (cell water) by Zerahn (1977). This average XMA concentration is also consistent with the mean K^+ activity of 95 ± 29 (SD) mM ($n = 74$) as measured with K^+-selective microelectrodes in the same tissue by Moffett, Hudson, Moffett and Ridgway (1982). The apparent K^+ activity coefficient of 0.71 is similar to that in other epithelia (*see* discussion below).

Electrical Evidence that K^+ Pump is on Apical Membrane

Using microelectrodes, Wood, Farrand and Harvey (1969) demonstrated a large, metabolism-dependent, PD step across the apical border of the midgut epithelium. However, PDs appear where high resistances are located and not necessarily where ion pumps are located (Schultz, 1972). Blankemeyer and Harvey (1977, 1978) identified two PD profiles from microelectrode impalements: a so-called HPD (High Potential Difference) profile identical with the profile of Wood et al. (1969) and a new LPD (Low Potential Difference) profile. They postulated that the LPD profile is from the K^+-transporting cell because both the apical resistance and the apical-to-basal resistance ratio of this LPD site increased when the tissue was subjected to anoxia and therefore that the K^+ pump is on the goblet cell apical membrane. However, dye iontophoretically injected into LPD sites was not recovered in histological sections of goblet cells. Later, Blankemeyer (1981) injected dye into HPD cells and recovered it in columnar cells but again recovered no dye from LPD injection sites. Recently, Moffett et al. (1982) injected dye into cells with PDs ranging from -20 to -95 mV and recovered it in both the columnar and the goblet cells. However, like Blankemeyer, they were unable to recover any dye injected into sites with PD less than -20 mV. Moffett et al. argued that the LPD sites are either in the basal extracellular space or in damaged goblet cells. The three microelectrode studies do show indirectly that the K^+ pump must be on the apical membranes of the epithelial cells because the cells are all more than 25 mV negative to the basal solution and 150 mV negative to the apical solution. Therefore if K^+ were pumped into the cells across the basal membrane it could not diffuse passively out of the cells against this large electrical gradient in the apical membrane. In summary, analysis of the electrical potential component of the electrochemical gradient, $\Delta\psi$, does show that the K^+ pump must be on the apical plasma membrane of columnar cells or of goblet cells.

XMA (Concentration) Evidence that K^+ Pump is on GCAM

The XMA technique lets us measure the chemical component of the electrochemical gradient with a resolution of approximately 0.5 μm. Because the midgut cells are large (30 to 40 μm wide by 50 to 100 μm tall) and because a large cavity (20 μm across) is located on the apical side of the goblet cells, XMA should tell us whether or not the K^+ pump is located on the GCAM. If the K^+ pump is located there then it must be pumping K^+ from the goblet cytoplasm to the goblet cavity; we might expect that the K concentration would be higher in the cavity than in the cytoplasm while the K^+ pump is operating; and we *must* find that the K concentration drops in the cavity when the K^+ pump is stopped. The crucial data then are (1) the K concentration in goblet cytoplasm and goblet cavity while the K^+ pump is operating (in oxygen) and the values in the same sites when the K^+ pump is stopped (in nitrogen).

The XMA data provide clear and direct evidence that the K^+ pump is indeed on the GCAM. As seen in Tables 1 and 2, and Fig. 7, when the K^+ pump is running (in oxygen) the K concentration is somewhat higher in the goblet apical projections and the goblet cavity than in the goblet cyto-

plasm. Most convincingly, when the K^+ pump was inhibited under anoxia, the K concentration in the goblet cavity was reduced from 200 to 68 mM, i.e. the apical concentration gradient was reversed. Thus the XMA data provides strong electrochemical evidence that the K^+ pump is on the GCAM. Incidentally, the XMA data neither support nor rule out an additional location of K^+ pumping sites on the columnar cell apical membrane because there is no isolated compartment apical to this membrane in which to detect a drop in K concentration when the pump is inhibited. The small drop in potassium concentration in the columnar cell brush border might result from a reduced rate of secretion by goblet cells; however, the converse is structurally improbable. Finally, the XMA data show that the largest K concentration increase is between basal extracellular space and goblet cytoplasm; this basal step was little affected by anoxia; we will discuss it further below.

XMA Evidence that LPD Sites are not in Goblet Cells

XMA allowed us to measure the K concentration within the goblet cells. The data establish without ambiguity that under four different steady-state conditions the goblet cells have the high K concentration usually characteristic of cells, including transporting epithelial cells of animals in general and of insects in particular (*see* Table 3 in Gupta and Hall, 1982). The average concentrations of intracellular K (expressed in mmol/kg wet weight) in goblet cells were: *in vivo* 103 ± 11 ($n=22$); *in vitro*, open circuit, 103 ± 12 ($n=21$); *in vitro*, short circuit, 132 ± 6 ($n=31$); and *in vitro*, short circuit under anoxia, 107 ± 11 ($n=19$). Out of some 175 intracellular sites sampled in goblet cells from 26 larvae we did not encounter a single site in which the K concentration even approached the low values (below 50 mM) expected if the goblet cells were the site of LPD impalements. These data thus support the recent microelectrode data of Moffett et al. (1982), who found the potassium activity of both columnar and goblet cells to be around 95 mM.

How is the High Cell K Maintained; Is Basal Entry Passive?

The XMA profile shows that the largest K step is from the basal extracellular fluid into the cytoplasm in both goblet and columnar cells (Tables 1 & 2 and Figs. 7 & 8). Is K^+ movement from blood side ECS to cells active or passive? Wood et al. (1969) argued that it is passive because the basal PD step increased from -25 to -75 mV when K^+ in the basal bathing solution was reduced from 32 to 2 mM. Moffett et al. (1982) showed that in cellular (HPD) impalement sites the K^+ activity is close to or slightly lower than the value required for electrochemical equilibrium across the basal cell membrane. A similar situation prevails in *Calliphora* salivary glands (Gupta et al., 1978). The Nernst equilibrium PD (E_K) calculated from the XMA data for K^+ across the basal cell membrane is -26 mV for goblet cells and is -31 mV for columnar cells (inside negative). Since the calculated E_K values in all studies agree so well with measured membrane PDs it is clear that K^+ is near equilibrium across the midgut cell basal membranes.

In the absence of an Na^+, K^+-ATPase in this tissue, Jungreis and Vaughan (1977) had suggested that the high level of intracellular K might be maintained by a "double-Donnan" equilibrium in which immovable, negatively charged macromolecules in the basal ECS balance Donnan effects of immovable negatively charged macromolecules within cells. However, before we accept the hypothesis that basal K^+ entry into midgut epithelial cells is passively regulated by a double-Donnan equilibrium, we must recall the nerve and muscle story and be cautious. K^+ is near equilibrium in these excitable cells but is not maintained passively even in excitable cells of insects; instead the Na^+ and K^+ gradients are the result of Na^+, K^+ pump activity and concomitant passive leaks. By a similar logic the observation that K^+ is virtually at equilibrium across the basal membranes does not rule out a basal K^+ pump. Cioffi has unpublished evidence that ^{42}K loads very slowly from the basal side in nitrogen whereas Harvey and Zerahn (1969) find rapid loading in oxygen. Harvey (1980) has suggested a metabolically dependent K^+/H^+ exchange across the basal cell membrane as part of the mechanism for alkalization of the gut lumen but no direct evidence exists for such a mechanism. The nature of basal K^+ entry remains uncertain and may most easily be resolved by studying the transport capabilities of the basal membrane fragments recently isolated by Cioffi and Wolfersberger (1983).

Enhanced K^+ Exchange During Anoxia

The average cell K in short-circuit samples is about 20 mM higher than in the other samples in both goblet and columnar cells (Table 4). This increase represents a 20% rise in cell K over open-circuit

and *in vivo* samples and is not accompanied by a corresponding loss in cell water. The calculated E_K values are now -40 mV for goblet cells and -41 mV for the columnar cells. Furthermore, under anoxia, when apical K^+ transport is inhibited and the accompanying short-circuit current is abolished, the average cell K reverts back to the baseline values. The drop is largely confined to the apical cytoplasm in the goblet cells (from 130 ± 5 mM K ($n=22$) to 91.8 ± 7 mM K ($n=11$)). If K is in equilibrium, this result implies that the cells become correspondingly hyperpolarized (cell more negative to basal solution) under short-circuit conditions and that concomitantly cell K rises and therefore the loading pool (^{42}K entering the tissue) would also rise. The increased K in goblet cells would account in part for the larger K pool under short-circuit conditions reported by Blankemeyer and Harvey (1978) but the major effect would be an enhanced coupling between goblet and columnar cells via the enhanced movement of ions between ECS and each of these cell types.

K^+ Transport Pool

The pattern of anoxia-induced changes in the distribution of K ions together with the evidence that the rapidly equilibrating LPD impalement sites are in the basal ECS rather than in the goblet cells, suggest that most (but not all) of the fast, kinetic (flux) pool of K transport might be extracellular. This pool would consist of K ions in all of the ECS in basal infolds separated from the blood side compartment by the basement membrane and feeding into the apical half of the goblet cell. The ions will be drawn into the apical cytoplasm of the goblet cells (including the organelle-free cytoplasmic "wall" of the goblet cavity) by the activity of the apical K pump and then will be moved into the goblet cavity. The K^+ ions in the goblet cell apical cytoplasm will not mix rapidly with the relatively "unstirred" organelle-rich nucleoendoplasm, which would be regulated by conventional cell homeostatic mechanisms, independently of that portion of the cytoplasm involved in the transport route. Such internal compartmentalization has been suggested in toad urinary bladder (DiBona, 1980), in frog skin (Voute, Møllgard & Ussing, 1975), in rabbit ileum (Gupta & Hall, 1979), and in several other transporting epithelia, including *H. cecropia* larval midgut (Møllgard & Rostgaard, 1980). On the exit side of the K^+ pump the K ions in the goblet cavity and in the unstirred ECS of the overlying apical brush border would also be part of the transport pool (Cioffi & Harvey, 1981). The total volume of this fast kinetic pool would be about 50% of the gross tissue volume and would equal the estimate for the sucrose ECS (Zerahn, 1975; 1977; Abramcheck, Blankemeyer & Harvey, 1980). Considering that it will include compartments with the highest K concentration in the tissue, the total K in the pool could easily equal the tissue (cell) K measured by chemical methods but the total tissue K pool will not ordinarily be involved and therefore will not be measured by kinetic flux methods. This model will explain the paradox that under short-circuit conditions the size of the rapidly mixing K flux pool matches the size of the relatively slow-mixing total tissue K (Zerahn, 1977; Harvey, 1980). Thus under short-circuit conditions the unlabeled columnar cell K could exchange with labeled K in the basal extracellular pool and hence a much larger size of the kinetically measured K flux pool would be observed.

Midgut K Transport Route

Figure 9 is a revised model for the K transport route, incorporating the changes required by the new XMA data. The steps identified below correspond to the numbered arrows in the Figure.

Step 1 – K^+ diffuses from the stirred blood side solution to the unstirred basal ECS; fixed negative charges in the basement membrane may elevate the K^+ concentration there, as in Malpighian tubules and salivary glands (Gupta, Hall, Maddrell & Moreton, 1976; Gupta et al., 1978).

Step 2 – K^+ enters the apical goblet cell cytoplasm from the basal ECS.

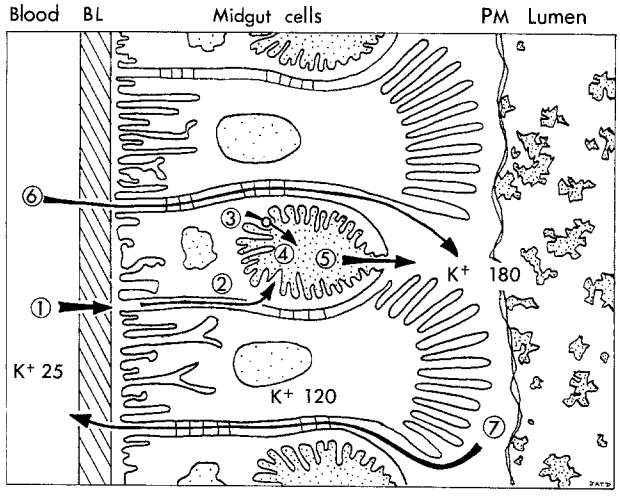

Fig. 9. Model for potassium transport in *Manduca sexta* midgut. *See* text for explanation. Abbreviations: *BL* = Basal Lamina, *PM* = Peritrophic Membrane. K^+ values are elemental potassium concentrations in mM

Step 3 – K^+ is actively and electrogenically transported from the apical goblet cell cytoplasm into the goblet cavity across the GCAM.

Step 4 – K^+ entering the goblet cavity is neutralized by fixed negative charges in the cavity matrix, and so: accompanying anion and water movement need not occur across GCAM, the cavity is thus electrically isolated, local back flux and shorting of the electrogenic pump PD is prevented, and the apical PD may be very high and approach the emf of the K^+ pump.

Step 5 – K^+ diffuses from goblet cavity to stirred solution in the lumen via a filtering valve (Flower & Filshie, 1976) which retains the large molecules.

Step 6 – Neutralizing anions, which pass from basal to apical side between the cells, join K^+ in the lumen.

Step 7 – *In vivo* (under open circuit) the large potassium ion concentration gradient (lumen high) and the electrical potential gradient (lumen positive) drive K^+ back to the blood side, between (and possibly through) the cells, and establish a K^+ pump-leak steady state. The high PD may be coupled to amino acid transport from lumen to blood (Nedergaard, 1977; Giordana, Sacchi & Hanozet, 1982). The paracellular flux would make the midgut "leaky" (low resistance) in spite of its paradoxically high TEP.

Ultrastructural changes observed when K^+ transport is turned off during moulting support this model (Cioffi, 1984). Zerahn's (1975, 1977) nonmixing pathway seems correct after all.

K^+ Pump and the Role of the Goblet Cavity

There are two other well-documented insect systems in which an electrogenic K^+ pump is localized on a highly folded, portasome-studded apical membrane and directed into a large cavity formed by the invagination of the apical cell surface: (a) the sensory sensilla of insects (Thurm & Küppers, 1980; Wieczorek, 1982) including the olfactory sensilla of moths *B. mori, A. pernyi* and *A. polyphemus* (Kaissling & Thorson, 1980; Steinbrecht, 1980); (b) the salivary glands of the blowfly *Calliphora* (Gupta et al., 1978; Berridge, 1980). In order to examine the possible role of the K^+-secreting system in the absorptive functions of the midgut and to understand the significance of a matrix-filled cavity, it is instructive to compare the key features of the three insect systems.

In sensory sensilla (Thurm & Küppers, 1980) the K^+ pump is located on the apical membranes of the tormogen and trichogen cells forming the receptor cavity. The transcellular (TEP) potentials can be >100 mV (cavity side positive). For the olfactory sensilla in moths (Kaissling & Thorson, 1980) with blood K at 36 mM the receptor lymph contained 200 mM K measured by flame photometry and had K^+ activity of 145 mM measured by K^+-sensitive microelectrodes. These values are remarkably similar to those found in the goblet cavity in our data. Even more uncanny is the close qualitative resemblance of X-ray energy spectra either from the micropuncture samples of the receptor lymph (Kaissling & Thorson, 1980) or from the XMA of cryosections (Steinbrecht & Zierold, 1982) to the spectra in Fig. 5 from goblet cells. In both tissues the cavity fluid contains high K, high sulfur but low Cl. Although quantitative results from XMA spectra of receptor cells have not been obtained, a Cl concentration of about 30 mM in the receptor lymph has been measured in other insects (Thurm & Küppers, 1980). The receptor lymph contains a specific protein in high concentration which on histochemical evidence is thought to be an acid glycosaminoglycan, presumably sulfated – hence the S-signal in the cavity (Kaissling & Thorson, 1980).

Thus it seems that both in sensory receptors and in the midgut goblet cells where a high TEP approaching the emf of the K^+ pump is sustained, the K^+-transport is directed into a cavity filled with (presumably) a sulfated glycoprotein providing some 50 to 100 meq/(kg wet wt) of fixed negative charge. This organic matrix with a net negative charge presumably acts as an extracellular Donnan system so that the amount of movable anions (Cl^-, OH^-, HCO_3^-) transferred across the GCAM down the PD gradient generated by K^+ pump is greatly reduced. Ultimately, anions must move, or K^+ be recycled, in order to maintain charge balance across the gut in the steady state. However, the matrix, combined with a high membrane resistance, would prevent these movements from reducing the potential developed across the transporting membrane itself.

This interpretation is supported by the data from *Calliphora* salivary glands. In this tissue the K concentrations (as well as activities) both on the cytoplasmic side and on the lumen side of the apical K^+ pump are about the same as in the lepidopteran receptors and goblet cells. In *Calliphora* salivary glands, however, the secretion of K^+ is accompanied by an equimolar transfer of Cl^- across the apical membrane (Gupta et al., 1978). The TEP is generally low (+15 mV under baseline

conditions and +2 mV after 5-hydroxytryptamine (5 HT) stimulation). However, if the secretion is stimulated by cAMP instead of 5-HT the TEP can rise up to 200 mV (lumen positive) but it begins to oscillate (Berridge, 1980, and *personal communication*). The interpretation is that cAMP can stimulate the K^+ pump but does not increase the Cl^- conductance of the apical membrane for which an increase in cell Ca^{2+} is needed. Thus in the absence of an extracellular matrix with a high density of negative charges, the high TEP generated by the K^+ pump cannot be sustained. In *Calliphora* salivary glands the electrogenicity of the K^+ pump is used not to sustain a high TEP, but to drive Cl^- and water fluxes, and produce an isotonic KCl fluid at high rates.

K^+ Pump and Midgut Function

Harvey (1980) has cogently argued that the function of K^+ secretion in the midgut of phytophagous lepidopteran larvae is to balance the K^+ absorption and hence maintain a constant K-level in the haemolymph. As was noted by Diamond and Bossert (1967), among others, the most efficient way to secrete ions (salt) without an accompanying movement of water would be to locate the ion pump on a membrane facing a large extracellular compartment (mucosal or serosal bulk fluid). However, the location of K^+ pumps in GCAM, directed into a semienclosed cavity with fixed negative charges is ill-suited to such a role; by analogy with the sensory sensillum, the cavity may thus be better suited to maintain the very high TEP generated by the primary activity of the electrogenic K^+ pump. The TEP (lumen positive) is then utilized to provide the potential energy for the absorption of sugars and amino acids, probably by cotransport with K^+ into the columnar cells (Nedergaard, 1977; Dow, Gupta & Hall, 1981; Giordana et al., 1982). It could also maintain a high pH in the gut lumen. Certain insect guts, characteristically those of lepidopteran larvae, contain fluid at a pH uniquely high in biological systems (in the present study, around pH 10.5). This is thought to represent an adaptation to tannin-rich plant foods (Berenbaum, 1980). The net TEP across the midgut *in vivo*, of 120 mV, would account for a passive ΔpH, across the gut, of 2 units. If the potential difference across the goblet cavity approached the emf calculated for the potassium ATPase (210 mV: Harvey, 1982), then the contents of the cavity could be at a pH 3.5 units higher than that of goblet cell cytoplasm. A secretion of alkali from the goblet cavity into the main gut lumen would thus account for the very high gut pH observed in lepidoptera, and explain the need to isolate electrically the potassium-transporting, goblet cavity membrane.

Conclusions

The XMA of frozen-hydrated and frozen-dried cryosections from the posterior midgut of *Manduca sexta* larvae has for the first time clearly demonstrated that under three steady-state conditions of K^+ transport: (a) the intracellular K is $\geqq 100$ mmol/(kg wet wt) both in the goblet cells and in the columnar cells; (b) highest levels of K (150 to 200 mM) are in the goblet cavity and the largest uphill gradient of K out of the cells is at the apical membrane of the goblet cells; and (c) the apical K gradient and the K contents of the goblet cavity are specifically reduced by 10 min of anoxia. Together with the previous evidence (Wolfersberger et al., 1982) the present work firmly locates the electrogenic K^+ pump on the portasome bearing apical membrane of the goblet cells. It is proposed that the function of an electrically isolated goblet cavity filled with an (acidic) organic matrix is to allow a much higher TEP, generated by the K^+ pump, to be maintained than would be possible across a flat surface. This high TEP is then used (a) to maintain passively a high pH (10 to 11) in the gut lumen and (b) to provide energy for the absorption of sugar and amino acids coupled to a downhill movement of K^+.

We would like to thank Mrs. J. Wardle and Mr. T. Burgess for their technical assistance; Mrs. J. Schreiber for assistance in preparing the manuscript and Drs. M. Cioffi and M.G. Wolfersberger for their helpful comments. We are most grateful to the staff of Temple University's workshops for their patient assistance during the development of the chamber. The Biological Microprobe Laboratory was established with a grant from the Science Research Council. The present work was supported by funds from Medical Research Council (U.K.), NIH Grant AI-09503, and Temple University's Research Incentive and Biomedical Research Funds. JATD is most grateful to the Commonwealth Fund for granting a three month leave of absence from his Harkness Fellowship and to St. Catharine's College, Cambridge, for allowing him to resume his Research Fellowship for June-August, 1982. TAH is a Leverhulme Research Fellow.

References

Abramcheck, F.J., Blankemeyer, J.T., Harvey, W.R. 1980. The size of the extracellular space in the isolated midgut of *Manduca sexta*. *J. Biol. Phys.* **8**:32–44

Anderson, E., Harvey, W.R. 1966. Active transport by the *cecropia* midgut. II: Fine structure. *J. Cell Biol.* **31**:107–134

Barnard, T. 1982. Thin frozen-dried cryosections in biological X-ray microanalysis. *J. Microsc. (Oxford)* **126**:317–332

Berenbaum, M. 1980. Adaptive significance of midgut pH in larval lepidoptera. *Am. Nat.* **115**:138–146

Berridge, M.G. 1980. The role of cyclic nucleotides and calcium in the regulation of chloride transport. *Ann. N.Y. Acad. Sci.* **341**:156–171

Blankemeyer, J.T. 1976. The route of active potassium transport in the midgut of *Hyalophora cecropia* and *Manduca sexta*. Ph.D. Thesis. Temple University, Philadelphia, Pa.

Blankemeyer, J.T. 1981. Association of microelectrode impalement potentials with morphologically distinguishable cell types in the insect midgut. *Physiologist* **24**:57 (Abstract)

Blankemeyer, J.T., Harvey, W.R. 1977. Insect midgut as a model epithelium. *In*: Water Relations in Membrane Transport in Plants and Animals. A.M. Jungreis, T.K. Hodges, A. Kleinzeller and S.G. Schultz, editors. Academic, New York

Blankemeyer, J.T., Harvey, W.R. 1978. Identification of active cell in potassium transporting epithelium. *J. Exp. Biol.* **77**:1–13

Brown, B.E. 1982. The form and function of metal-containing 'granules' in invertebrate tissues. *Biol. Rev. Camb. Philos. Soc.* **57**:621–667

Cioffi, M. 1979. The morphology and fine structure of the larval midgut of a moth *Manduca sexta* in relation to active ion transport. *Tissue Cell* **11**:467–479

Cioffi, M. 1984. Comparative ultrastructure of arthropod transporting epithelia. *Am. Zool.* (*in press*)

Cioffi, M., Harvey, W.R. 1981. Comparison of potassium transport in three structurally distinct regions of the midgut. *J. Exp. Biol.* **91**:103–116

Cioffi, M., Wolfersberger, M.G. 1983. Isolation of separate apical, lateral and basal plasma membrane from cells of an insect epithelium. A procedure based on tissue organisation and ultrastructure. *Tissue Cell* (*in press*)

Coles, J.A., Tsacopoulos, M. 1979. Potassium activity in photoreceptors, glial cells and extracellular space in the drone retina: Changes during phagostimulation. *J. Physiol. (London)* **290**:525

Diamond, J., Bossert, W.H. 1968. Standing-gradient osmotic flow. A mechanism for coupling of water and solute transport in epithelia. *J. Gen. Physiol.* **50**:2061–2083

DiBona, D.R. 1980. Cellular consequences of ADH-induced water flow. *In*: Water Transport Across Epithelia. Barriers, Gradients and Mechanisms. H.H. Ussing, N. Bindslev, N.A. Lassen and O. Sten-Knudsen, editors. pp. 437–453. Munksgaard, Copenhagen

Dow, J.A.T., Gupta, B.L., Hall, T.A. 1981. Microprobe analysis of Na, K, Cl, P, S, Ca, Mg and H_2O in frozen-hydrated sections of the anterior caecum of the locust, *Schistocerca gregaria*. *J. Insect Physiol.* **27**:629–639

Flower, N.E., Filshie, B.K. 1976. Goblet cell differentiation in the midgut of a lepidopteran larva. *J. Cell Sci.* **20**:357–375

Giordana, B., Sacchi, F. 1977. Some ionic and electrical parameters of the intestinal epithelium in the mature larvae of lepidoptera. *Comp. Biochem. Physiol.* **56A**:95–99

Giordana, B., Sacchi, F.V., Hanozet, G.M. 1982. Intestinal amino-acid absorption in lepidopteran larvae. *Biochim. Biophys. Acta* **692**:81–88

Gupta, B.L. 1976. Water movement in cells and tissues. *In*: Perspectives in Experimental Biology. P. Spencer-Davies, editor. Vol. I, pp. 25–42. Pergamon, Oxford

Gupta, B.L., Berridge, M.J. 1966. A coat of repeating subunits on the cytoplasmic surface of the plasma membrane in the rectal papillae of the blowfly, *Calliphora erythrocephala* Meig. studied *in situ* by electron microscopy. *J. Cell Biol.* **29**:376–382

Gupta, B.L., Berridge, M.J., Hall, T.A., Moreton, R.B. 1978. Electron microprobe and ion selective microelectrode studies of fluid secretion in the salivary glands of *Calliphora*. *J. Exp. Biol.* **72**:261–284

Gupta, B.L., Hall, T.A. 1978. Electron probe X-ray microanalysis of calcium. *Ann. N.Y. Acad. Sci.* **307**:28–51

Gupta, B.L., Hall, T.A. 1979. Quantitative electron probe X-ray microanalysis of electrolyte elements within epithelial tissue compartments. *Fed. Proc.* **38**:144–153

Gupta, B.L., Hall, T.A. 1981. The X-ray microanalysis of frozen-hydrated sections in scanning electron microscopy: An evaluation. *Tissue Cell* **13**:623–643

Gupta, B.L., Hall, T.A. 1982. Electron probe X-ray microanalysis. *In*: Techniques in Cellular Physiology, P.F. Baker, editor. Vol. P1/11, pp. P128/1-52. Elsevier/North Holland, County Clare

Gupta, B.L., Hall, T.A., Maddrell, S.H.P., Moreton, R.B. 1976. Distribution of ions in a fluid transporting epithelium determined by electron-probe X-ray microanalysis. *Nature (London)* **264**:284–287

Gupta, B.L., Hall, T.A., Moreton, R.B. 1977. Electron probe X-ray microanalysis. *In*: Transport of Water and Ions in Animals. B.L. Gupta, R.B. Moreton, J.L. Oschman and B.J. Wall, editors. pp. 83–143. Academic, London

Hall, T.A. 1971. The microprobe assay of chemical elements. *In*: Physical Techniques in Biological Research. 2nd edition. G. Oster, editor. Vol. 1A, pp. 157–275. Academic, New York

Hall, T.A., Gupta, B.L. 1979. EDS quantitation and application to biology. *In*: Introduction to Analytical Electron Microscopy. J. Hren, J. Goldstein and D. Joy, editors. pp. 169–197. Plenum, New York

Hall, T.A., Gupta, B.L. 1982*a*. The imaging problem in the X-ray microanalysis of matrix-free extracellular spaces in frozen-hydrated tissue sections. *In*: 40th Annu. Proc. Electron Microsc. Soc. Amer. G.W. Bailey, editor. pp. 394–397. Clairters, Baton Rouge

Hall, T.A., Gupta, B.L. 1982*b*. Quantification for the X-ray microanalysis of cryosections. *J. Microsc. (Oxford)* **126**:333–345

Harvey, W.R. 1980. Water and ions in the gut. *In*: Insect Biology in the Future "VBW 80". M. Locke and D.S. Smith, editors. pp. 105–124. Academic, London

Harvey, W.R. 1982. Membrane physiology of insects. *In*: Membrane Physiology of Invertebrates. R.P. Podesta and S.F. Timmers, editors. pp. 495–565. Marcel Dekker, New York

Harvey, W.R. Cioffi, M., Dow, J.A.T., Wolfersberger, M.G. 1983. Potassium ion transport ATPase in insect epithelia. *J. Exp. Biol.* **106**:91–117

Harvey, W.R., Cioffi, M., Wolfersberger, M.G. 1981. Portasomes as coupling factors in active ion transport and oxidative phosphorylation. *Am. Zool.* **21**:775–791

Harvey, W.R., Cioffi, M., Wolfersberger, M.G. 1983. Chemiosmotic potassium ion pump of insect epithelia. *Am. J. Physiol.* **244**:R163–R175

Harvey, W.R., Nedergaard, S. 1964. Sodium independent active transport of potassium in isolated midgut of the cecropia silkworm. *Proc. Natl. Acad. Sci. USA* **51**:757–765

Harvey, W.R., Wolfersberger, M.G. 1979. Mechanism of inhibition of active potassium transport in isolated midgut of *Manduca sexta* by *Bacillus thuringiensis* endotoxin. *J. Exp. Biol.* **83**:293–304

Harvey, W.R., Wood, J.L., Quatrale, R.P., Jungreis, A.M. 1975. Cation distributions across the larval and pupal midgut of the lepidopteran. *Hyalophora cecropia, in vivo*. *J. Exp. Biol.* **63**:321–333

Harvey, W.R., Zerahn, K. 1969. Kinetics and route of active K-transport in the isolated midgut of *Hyalophora cecropia*. *J. Exp. Biol.* **50**:297–306

House, C.R. 1980. Physiology of invertebrate salivary glands. *Biol. Rev.* **55**:417–473

Jungreis, A.M. 1978. The composition of the larval-pupal moulting fluid in the tobacco hornworm *Manduca sexta*. *J. Insect Physiol.* **24**:65–73

Jungreis, A.M., Vaughan, G.L. 1977. Insensitivity of lepidopteran tissues to ouabain: Absence of ouabain binding and Na^+,K^+ ATPase in larval and adult midgut. *J. Insect Physiol.* **23**:503–507

Kaissling, K.E., Thorson, J. 1980. Insect olfactory sensila: Structural, chemical and electrical aspects of the functional organisation. *In*: Receptors for Neurotransmitters, Hormones and Pheremones in Insects. D.B. Sattelle, editor. Elsevier/North Holland, Amsterdam

Keynes, R.D. 1969. From frog skin to sheep rumen: A survey of transport of salts and water across multicellular structures. *Quart. Rev. Biophys.* **2**:177–281

Maddrell, S.H.P. 1980. Characteristics of epithelial transport in insect Malpighian tubules. *Curr. Top. Membr. Transp.* **14**:427–463

Mandel, L.J., Riddle, T.G., Storey, J.M. 1980. Role of ATP in respiratory control and active transport in tobacco hornworm midgut. *Am. J. Physiol.* **238**:C10–C14

Moffett, D.F. 1979. Bathing solution tonicity and potassium transport by the midgut of the tobacco hornworm *Manduca sexta*. *J. Exp. Biol.* **78**:213–223

Moffett, D.F., Hudson, R.L., Moffett, S.B., Ridgway, R.L. 1982. Intracellular K^+ activities and cell membrane potentials in a K^+-transporting epithelium, the midgut of tobacco hornworm (*Manduca sexta*). *J. Membrane Biol.* **70**:59–68

Mollgard, K., Rostgaard, J. 1980. The transcellular compartment of tubulo-cisternal endoplasmic reticulum, a common feature of transporting epithelial cells. *In*: Water Transport Across Epithelia. Barriers, Gradients and Mechanisms. H.H. Ussing, N. Bindslev, N.A. Lassen and O. Sten-Knudsen, editors. pp. 85–101. Munksgaard, Copenhagen

Nedergaard, S. 1977. Amino-acid transport. *In*: Transport of Ions and Water in Animals. B.L. Gupta, R.B. Moreton, J.L. Oschman and B.J. Wall, editors. pp. 239–264. Academic, London

Phillips, J.E. 1980. Epithelial transport and control in recta of terrrestrial insects. *In*: Insect Biology in the Future "VBW 80". M. Locke and D.S. Smith, editors. pp. 145–177. Academic, New York

Ramsay, J.A., Brown, R.H.J., Croghan, P.C. 1955. Electrometric titration of chloride in small volumes. *J. Exp. Biol.* **32**:822–829

Schultz, S.G. 1972. Electrical potential differences and electromotive forces in epithelial tissues. *J. Gen. Physiol.* **59**:794–798

Somlyo, A.V., Silcox, J. 1979. Cryoultramicrotomy for electron probe analysis. *In*: Microbeam Analysis in Biology. C.P. Lechene and R.R. Warner, editors. pp. 535–555. Academic, New York

Somlyo, A.P., Somlyo, A.V., Shuman, H. 1979. Electron probe analysis of vascular smooth muscle: Composition of mitochondria, nuclei and cytoplasm. *J. Cell Biol* **81**:316–335

Steinbrecht, R.A. 1980. Cryofixation without cryoprotectants. Freeze substitution and freeze etching of an insect olfactory receptor. *Tissue Cell* **12**:73–100

Steinbrecht, R.A., Zierold, K. 1982. Cryo-embedding of small frozen specimens for cryo-ultramicrotomy. *In*: 10th Int. Congr. Electron Microsc. Hamburg, August 17–24, 1982. pp. 183–184

Thurm, U., Küppers, J. 1980. Epithelial physiology of insect sensilla. *In*: Insect Biology in the Future "VBW 80". M. Locke and D.S. Smith, editors. pp. 735–763. Academic, New York

Turbeck, B.O. 1974. A study of the concentrically laminated concretions, 'Spherites,' in the regenerative cells of the midgut of lepidopterous larvae. *Tissue Cell* **6**:627–640

Voute, C.L., Mollgaard, K., Ussing, H.H. 1975. Quantitative relationship between active sodium transport, expansion of endoplasmic reticulum and specialized vacuoles ("scalloped sacs") in the outermost living cell layer of the frog skin epithelium (*Rana temporaria*). *J. Membrane Biol.* **31**:273–289

Wieczorek, H. 1982. A biochemical approach to the electrogenic potassium pump of insect sensilla: Potassium sensitive ATPases in the labellum of the fly. *J. Comp. Physiol.* **21**:273–289

Wolfersberger, M.G., Harvey, W.R., Cioffi, M. 1982. Transepithelial potassium transport in insect midgut by an electrogenic alkali metal ion pump. *Curr. Top. Membr. Transp.* **16**:109–133

Wood, J.L., Farrand, P.S., Harvey, W.R. 1969. Active transport of potassium by the *cecropia* midgut. VI. Microelectrode potential profile. *J. Exp. Biol.* **50**:169–178

Wood, J.L., Moreton, R.B. 1978. Refinements in the short-circuit technique and its applications to active potassium transport across the *cecropia* midgut. *J. Exp. Biol.* **77**:123–140

Zerahn, K. 1975. Potassium exchange between bathing solution and midgut of *Hyalophora cecropia* and time delay for potassium flux through the midgut. *J. Exp. Biol.* **63**:295–300

Zerahn, K. 1977. Potassium transport in insect midgut. *In*: Transport of Water and Ions in Animals. B.L. Gupta, R.B. Moreton, J.L. Oschman and B.J. Wall, editors. pp. 381–401. Academic, London

Received 11 April 1983; revised 14 July 1983